Cysteine-Scanning Mutagenesis of Flanking Regions at the Boundary between External Loop I or IV and Transmembrane Segment II or VII in the GLUT1 Glucose Transporter†

Andreas Olsowski, Ingrid Monden, and Konrad Keller*

Institut für Pharmakologie, Freie Universität Berlin, Thielallee 67-73, D-14195 Berlin, FRG

Received February 24, 1998; Revised Manuscript Received April 30, 1998

ABSTRACT: To investigate local secondary structure of GLUT1, site-directed and cysteine-scanning mutagenesis were employed to probe *p*-chloromercuribenzenesulfonate sensitivity of flanking regions at the boundary of external loops (ELs) and transmembrane segments (TMs) and to check the compatibility of two alternative membrane topology models with the experimental data. In the Cys-less GLUT1, single serine residues located in external loops adjacent to putative transmembrane segments were replaced with cysteine. Transport activities of the cysteine-replacement mutants were comparable to that of the nonmutated Cys-less GLUT1. Only the cysteine residues inserted into the first or fourth EL contributed to transport inhibition by *p*-chloromercuribenzenesulfonate (pCMBS). Dependent on the pCMBS sensitivity of these residues, cysteine-scanning mutagenesis of flanking regions was performed, including EL I−TM II and TM VII−EL IV, respectively. Of the 27 amino acids changed, the majority of cysteine-substitution mutants displayed transport activities comparable to that of Cys-less GLUT1. Irreplaceable amino acids were Phe-72, Gly-286, Asp-288, Tyr-292, and Tyr-293. The pCMBS sensitivity of loop residues decreased when the distance between inserted thiol groups and the putative transmembrane limit increased. The mutants T62C, T63C, T295C, and I297C even exhibited transport stimulation after pCMBS treatment. Regarding putative membrane-harbored residues, a few thiol groups were involved in pCMBS-induced transport inhibition. Drawn on a helix wheel, these pCMBS-sensitive cysteine residues lie on the same facial half of the helix, shown for TM II and TM VII. With respect to EL−TM boundaries, the experimental data are consistent with the local secondary structure predicted from hydropathy profiles. Conversely, certain data obtained by pCMBS-sensitivity scanning are not consistent with either of the two recently published alternative GLUT1 topology models.

A growing body of evidence suggests that the polypeptide arrangements of members of the facilitative glucose transporter family consist of 12 putative transmembrane segments, composed mainly of α-helices (*1*). Primarily based on hydropathy profiles, this topology remains unverified, and in particular, the exact end points of the transmembrane stretches are still uncertain. Recently, two alternative topographic assignments of GLUT1 have been presented that, in contrast to the 12 spanning segments, favor a secondary structure with 16 *β*-strands, resembling the bacterial porin protein (*2*), or an α-helix−*β*-strand transmembrane structure with 14 membrane-spanning segments (*3*).

An important contribution to the elucidation of the secondary structure of GLUT1 came from experiments which by proteolytic digestion and use of site-specific antipeptide antibodies confirmed that both the carboxyl terminus and the large hydrophilic loop face the cytoplasm (*4*, *5*). Asn-45 which is located in the external loop (EL)[1] connecting putative transmembrane segments (TM) I and II was identified as the site of glycosylation (*4*). Further insight into local secondary structure was achieved with labeling experiments using a membrane-impermeant lysine-specific reagent (isethionyl acetimidate) together with proteolytic digestion of the transporter protein. In a C-terminal tryptic fragment, Lys-300 was identified as the exofacially labeled residue, consistent with it being located in an external loop (*6*). The extramembranous localization of this lysine residue was also predicted by each of the alternative membrane topology models.

Among the three cysteine residues of a 19 kDa carboxyl-terminal cleavage fragment of human red cell glucose transporter, Cys-429 was considered to be the most likely candidate for exofacial binding to an external ligand (*7*). In single-cysteine mutation experiments, the absence of reactivity of the remaining thiol groups with the membrane-impermeant reagent *p*-chloromercuribenzenesulfonate (pC-

† This work was supported by the Deutsche Forschungsgemeinschaft (Grant Ke 390/6-1).

* To whom correspondence should be addressed at Institut für Pharmakologie, Freie Universität Berlin, Thielallee 67-73, D-14195 Berlin, FRG. Telephone: +49-30-8383315. Fax: +49-30-8315954. E-mail: Kellerfu@zedat.fu-berlin.de.

[1] Abbreviations: NEM, *N*-ethylmaleimide; pCMBS, *p*-chloromercuribenzenesulfonate; 2-DOG, 2-deoxy-D-[2,6-^{3}H]glucose; 3-OMG, 3-*O*-methyl-D-[1-^{3}H]glucose; EL, extracellular loop; TM, transmembrane segment; MBS, Barth's modified saline solution.

S0006-2960(98)00440-1 CCC: $15.00 © 1998 American Chemical Society
Published on Web 07/09/1998

MBS) supported this notion. Cysteine at position 429 presumably is the only cysteine residue of GLUT1 that is accessible to pCMBS from the outside, leading to transport inhibition (*8*). This notion was confirmed by recent experiments on GLUT4-mediated transport which was inhibited by pCMBS if Met-455, corresponding to Cys-429 of GLUT1, was changed to a cysteine residue (*9*). It is worth noting that all three topological models agree about the extracellular location of Cys-429. Recent data obtained from an elegant approach using an aglyco-GLUT1 construct and analyzing membrane topology by glycosylation-scanning mutagenesis strongly supports the 12-helix model (*10*).

Site-directed and cysteine-scanning mutagenesis have proved to be a powerful procedure for investigating the secondary structure of *Escherichia coli* lactose permease (for TM II and VII, see refs *11* and *12*). These studies also showed that only a few amino acid residues were irreplaceable with respect to active transport. In further assays, the majority of cysteine-substitution mutants could thus be tested with respect to transport inhibition by the alkylating agent NEM. Our goal was to investigate membrane topology motifs at the interface between external loops and transmembrane segments in GLUT1 and to identify the amino acid residues that form the end points at the boundary between loop and membrane segments. Confirmed by independent groups, the cysteine-less version of GLUT1 (Cys-less GLUT1) functioned as an active transport protein (*13*−*15*). Thus, a combination of site-directed and cysteine-scanning mutagenesis of Cys-less GLUT1 was employed, together with assessment of the pCMBS and NEM sensitivities of inserted single thiol groups.

Data from glycosylation-scanning mutagenesis demonstrated that insertion of a glycosylated domain into each of the external loops of the aglyco-GLUT1 did not impair transport activity for all events (*10*). The most probable explanation was that exofacial loops whose manipulation did not affect transport activity may not be essentially involved in the transport process. Therefore, it seemed reasonable to test first the pCMBS sensitivity of loop thiol groups that replaced serine residues adjacent to the flanking transmembrane segment in question. If inhibition of a mutant was greater than 50%, cysteine-scanning mutagenesis of flanking regions was performed. The pCMBS reactivity of inserted SH groups would indicate a location on the outer face of the membrane or a position within the membrane helix that is accessible to hydration water. Since the transmembrane helix length of membrane proteins reportedly is on average more than 20 amino acid residues (*16*), cysteine-scanning mutagenesis of the defined amino acid stretch included exofacial loop residues and transmembrane amino acids.

Experimental evidence that supported the following conclusions was obtained. (a) Only the serine residues substituted in the first and fourth external loops led to marked pCMBS-induced transport inhibition. (b) When inserted into putative membrane-spanning segments, a few cysteine residues were sensitive to inhibition by membrane-impermeant pCMBS. (c) The results of cysteine-scanning mutagenesis of flanking regions, including the first EL−second TM or the seventh TM−fourth EL boundary, were consistent with the local secondary structure predicted from hydropathy analysis. (d) Inconsistency between the alternative topological models and the experimental data contributes to a better prediction of the GLUT1 structure.

MATERIALS AND METHODS

Materials. The oligonucleotides for mutagenesis were from GibcoBRL (Life Technologies, Eggenstein, FRG); the radiolabeled glucose analogues (2-deoxy-D-[2,6-^{3}H]glucose, with a specific activity of 26.2 Ci/mmol, and 3-*O*-methyl-D-[1-^{3}H]glucose, with a specific activity of 2.5 Ci/mmol) were from Amersham Buchler (Braunschweig, FRG). NEM and pCMBS were from Sigma (Deisenhofen, FRG). Female *Xenopus laevis* frogs were from the African Xenopus Facility CC (Knysna, Republic of South Africa).

Mutagenesis and cRNA Preparation. A 2.4 kb *Bam*HI fragment of human GLUT1 cDNA derived from pSPGT (*17*) was subcloned into a *Bgl*II site of the *Xenopus* oocyte expression vector pSP64T (*18*). This construct served as a template for generating a Cys-less GLUT1 construct as described previously (*14*). Site-directed mutagenesis of the Cys-less GLUT1 was conducted according to the procedure of Deng and Nickoloff (*19*) using a mutagenesis kit provided by Pharmacia (Pharmacia Biotech, Freiburg, FRG). A single serine residue in each of the external loops (I−V) was changed to cysteine to localize those positions that are sensitive to pCMBS treatment. Dependent on pCMBS sensitivity, cysteine-scanning mutagenesis of two amino acid stretches was performed, each containing five loop residues and eight or nine residues harbored in transmembrane segments. Mutations were confirmed by restriction fragment analysis and finally by DNA sequence analysis with a fluorescence 377 DNA Sequencer (ABI PRISM) connected to a Macintosh computer.

In vitro cRNAs synthesis of Cys-less GLUT1 or Cys-replacement mutants was conducted with the *Xba*I-linearized plasmid templates using the mMESSAGE mMACHINE transcription kit (AMBION, Austin, TX). After purification of the newly transcribed cRNAs with the RNeasy system (QIAGEN, Hilden, FRG), the amount of cRNA was calculated by counting the radioactivity of incorporated [^{35}S]thio-UTP and, in addition, by determination of the 260 nm:280 nm absorbance ratio with a spectrophotometer.

Xenopus Oocyte Isolation and Determination of Transport Activity. Collection, defolliculation, and culture of *Xenopus* oocytes as well as cRNA injection into the cells were carried out routinely as reported previously (*20*, *21*).

Tritium-labeled 2-deoxy-D-glucose (50 μM, 1 μCi/0.5 mL transport assay) or 3-*O*-methyl-D-glucose (1 mM, 5 μCi/0.5 mL transport assay) was used as the glucose analogue for uptake determination. In an independent experiment, each group included 20 to 30 *Xenopus* oocytes expressing Cys-less GLUT1 or various Cys-replacement mutants; the transport assay contained 10−15 single oocytes in 0.5 mL of Barth's modified saline solution (MBS). A comparable number of water-injected *Xenopus* oocytes served as a control to indicate the translational efficiency of the cRNA-injected group. After incubation for 30 min with 2-deoxy-D-glucose (2-DOG) or for 5 min with 3-*O*-methyl-D-glucose (3-OMG) (linear range of uptake for each substrate), uptake of glucose analogues was terminated by washing the oocytes four times with 3 mL of ice-cold phosphate-buffered saline containing 0.1 mM phloretin as the transport inhibitor. Oocytes were

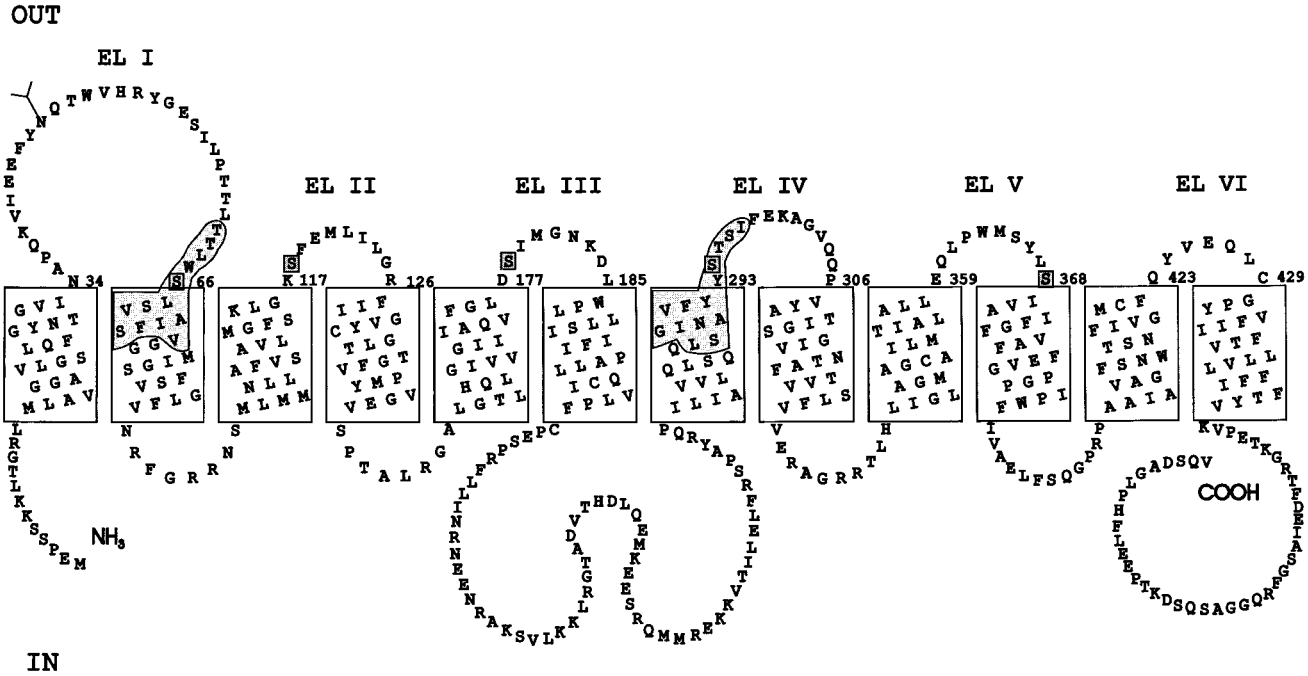

FIGURE 1: Twelve-helix membrane topology model of GLUT1. Amino acids of GLUT1 are indicated by their single-letter code. According to the secondary structure predicted from the hydropathy profile, the putative transmembrane segments are shown in boxes. The shaded regions highlight those amino acids and domains that are included in site-directed (S in a box) and cysteine-scanning mutagenesis (shaded area). Positions that mark the end point residues of external loops are numbered. The six external loops are designated EL I−VI.

individually transferred into scintillation vials and dissolved by adding 0.5 mL of 1% SDS before the radioactivity was determined. Uptake rates were expressed as picomoles of accumulated 2-DOG or 3-OMG per oocyte per minute.

If cysteine substitution led to low transport activities (i.e., 2-DOG uptake of <20% of Cys-less GLUT1), uptake rates were normalized to the relative amount of the mutant transporter protein expressed in total membrane fractions. On the basis of dot-blot analysis, as previously described in detail (*22*), radioactivity was determined with a BAS-1500 PhosphoImager (FUJIFILM) and TINA software, version 2.09f (Raytest-Isotopenmessgeräte). Comparison of transport activities was made by calculating the ratio of (mean uptake rate/relative amount of the particular Cys-replacement mutant) to (mean uptake rate/relative amount of Cys-less GLUT1).

Transport Inhibition by pCMBS and NEM. Inhibition experiments were carried out by using the membrane-impermeant pCMBS and the membrane-permeable NEM that covalently binds to SH groups. In the NEM-induced transport inhibition studies, *Xenopus* oocytes were incubated with 10 mM NEM for 60 min. This concentration was chosen because prior testing indicated that NEM is not a very effective inhibitor of GLUT1 expressed in *Xenopus* oocytes. Following NEM preincubation, 3-OMG uptake rates were shown to be the same whether NEM was present or absent in the transport assay. For experiments with the membrane-impermeant pCMBS, *Xenopus* oocytes were incubated for 60 min before 2-DOG uptake was measured for 30 min in the presense of the inhibitor. Five concentrations of pCMBS (increasing from 0.5 to 2.5 mM) were tested with respect to inhibition of Cys-less GLUT1-induced 2-DOG uptake. Subtraction of uptake rates by the water-injected *Xenopus* oocytes was always mandatory since pCMBS was a very effective inhibitor of the oocyte endogenous hexose transport system. To assess the pCMBS sensitivity of Cys-replacement mutants, the rather high concentration of 2 mM for pCMBS was chosen. To take into account all uptake rates determined for a particular Cys-replacement mutant obtained from independent experiments, values of single inhibitor-treated *Xenopus* oocytes were calculated as a percentage of the mean uptake rate of the corresponding untreated group.

RESULTS

Substitution of Single Loop Serine Residues in Cys-less GLUT1. To probe the interface between external loops and transmembrane segments, we used a strategy which combined single serine mutations at particular positions of external loops, cysteine-scanning mutagenesis, and modification of inserted thiol groups by sulfhydryl reagents. pCMBS at concentrations increasing from 0.5 to 2.5 mM did not affect 2-deoxy-D-glucose uptake, whereas NEM at 10 mM reduced the catalytic activity of the Cys-less GLUT1 by about 30% (data not shown).

In the first step, single serine residues within external loops adjacent to flanking membrane-spanning segments were replaced with cysteines by site-directed mutagenesis. Consistent with the 12-helix membrane topology, five out of six external loops (I−V) were individually modified by introducing single thiol groups at positions that are indicated in Figure 1. Presumably due to the structural similarity between serine and cysteine residues, cysteine substitution led only to minor changes in transport activities, as documented for mutants S66C, S118C, S178C, S294C, and S368C (depicted in Figure 2). Sensitivities to pCMBS, however, were quite different. Mutants S66C and S294C carrying SH groups in the first or fourth EL displayed 2-deoxy-D-glucose uptake rates that were only 9 and 7% of that of the untreated group. Cysteine at position 368 was less sensitive to pCMBS,

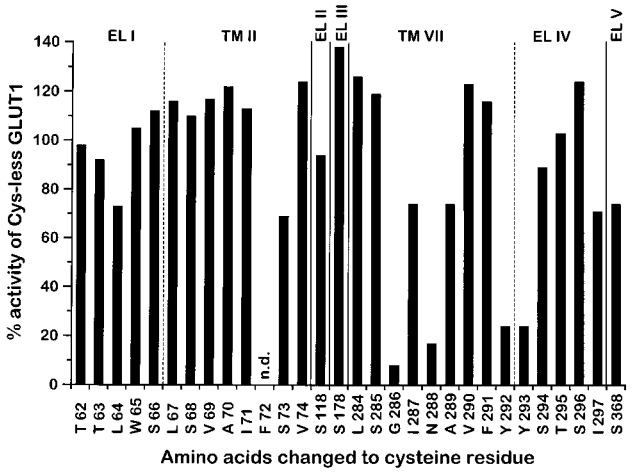

FIGURE 2: Relative 2-deoxy-D-glucose uptake rates of cysteine-replacement mutants. Uptake of tritium-labeled 2-deoxy-D-glucose was assessed in *Xenopus* oocytes expressing the Cys-less GLUT1 or the indicated Cys-replacement mutants of the Cys-less GLUT1. *Xenopus* oocytes were injected with identical amounts of cRNA. Taken from numerous independent experiments, a representative mean uptake rate by the Cys-less GLUT1 of 2-deoxy-D-glucose was 3.15 ± 0.37 pmol of 2-DOG oocyte^{-1} min^{-1}. Each bar indicates the mean uptake rate of a particular Cys-substitution mutant expressed as percentage of that of the Cys-less GLUT1 in the same experiment. Calculation of each mean included 20−30 single *Xenopus* oocytes. n.d. means not detected.

leading to 18% transport reduction. The cysteine residues inserted into the second or third EL were resistant with respect to transport inhibition by pCMBS.

Cysteine-Scanning Mutagenesis of the First EL−Second TM Region. Due to the effective transport inhibition by pCMBS modification of membrane-adjacent thiol groups within the first and fourth external loops, we decided to investigate local secondary structure at the interface between these loops and adjoining transmembrane segments by performing cysteine-scanning mutagenesis. Regarding the flanking regions at the first EL−second TM boundary, cysteine-scanning mutagenesis started from serine at position 66, which is predicted to be the end point at the C-terminal end of the loop, and was extended toward the C and N termini of the protein (as shown in Figure 1). Single thiol groups were inserted into an amino acid stretch that contained five residues of the first EL and eight residues of the second TM at its N-terminal end. Figure 2 shows that within this domain only phenylalanine at position 72 appeared to be irreplaceable with respect to transport activity, so that for the majority of mutants the pCMBS sensitivity and transport inhibition could be assessed. If the low uptake rate of the F72C mutant was normalized to the relative amount of the mutant protein in the total membrane fraction, transport activity was 8% of that of the nonmutated Cys-less GLUT1 (for details, see Materials and Methods).

The data in Table 1 demonstrate that pCMBS-sensitivity scanning of thiol groups at the first external loop identified S66C as the most sensitive mutant, displaying 9% remaining transport activity after pCMBS treatment. Sensitivities of the other loop cysteine residues decreased with increasing distance by number from the flanking transmembrane segment. It is worth noting that the two cysteine residues that are farthest from the membrane site (i.e., Cys-63 and Cys-62) even led to a modest stimulation of transport after pCMBS treatment (141 and 130%, respectively).

Table 1: Effect of pCMBS on Cys-Replacement Mutants[a]

region	Cys-replacement mutants	% activity ± SD	no. of oocytes
first EL	T62C	130 ± 35	85
	T63C	141 ± 30	79
	L64C	95 ± 41	83
	W65C	38 ± 31	69
	S66C	9 ± 5	95
second TM	L67C	94 ± 27	66
	S68C	93 ± 23	80
	V69C	70 ± 17	71
	A70C	4 ± 7	70
	I71C	101 ± 29	96
	F72C	nd	51
	S73C	3 ± 2	49
	V74C	108 ± 30	69
second EL	S118C	93 ± 40	76
third EL	S178C	114 ± 53	71
seventh TM	L284C	97 ± 25	89
	S285C	95 ± 22	95
	G286C	303 ± 190	69
	I287C	7 ± 5	70
	N288C	14 ± 10	87
	A289C	78 ± 23	49
	V290C	44 ± 19	70
	F291C	9 ± 4	77
	Y292C	88 ± 29	63
fourth EL	Y293C	42 ± 18	52
	S294C	7 ± 4	78
	T295C	140 ± 43	99
	S296C	91 ± 34	86
	I297C	323 ± 169	99
fifth EL	S368C	82 ± 18	90

[a] Water-injected *Xenopus* oocytes and oocytes expressing single-cysteine mutants were incubated with 2 mM pCMBS at room temperature for 60 min. Thereafter, uptake of tritium-labeled 2-deoxy-D-glucose was assessed as described in Materials and Methods. For each single-cysteine-replacement mutant, the retained transport activity after pCMBS treatment was expressed as a percentage of the 2-deoxy-D-glucose uptake rate in absence of pCMBS. Uptake rates obtained from water-injected *Xenopus* oocytes were subtracted. For single-Cys-replacement mutants, values are the mean percentage ± standard deviation of retained uptake rates and the total number of single *Xenopus* oocytes from three or four independent experiments. nd means not detected.

Among the active cysteine-replacement mutants whose thiol groups are predicted to be located in the second TM, a few displayed sensitivity to pCMBS (Table 1). Uptake rates of mutants V69C, A70C, and S73C were inhibited by 30, 96, and 97%, respectively, indicating that the inserted intramembranous SH groups were exposed to hydration water or water held by cavities containing the sulfhydryl-reactive agent. With respect to the EL−TM boundary, it was particularly important that the residue at position 67, which is predicted to be the N-terminal end point of the second TM, was not involved in pCMBS-induced transport inhibition (94% retained transport activity), in contrast to the pCMBS-sensitive cysteine at position 66 that is predicted to form the C-terminal limit of the first external loop. When the membrane-localized residues are plotted on a helical wheel (Figure 3), pCMBS-sensitive residues within this portion of the second TM lie on one face of the helix. The entire amino acid stretch, including residues 62−72, is predicted to be part of the second TM in both alternative membrane topologies. In the 16-strand model, the following two positions, i.e., Ser-73 and Val-74, are proposed to be part of

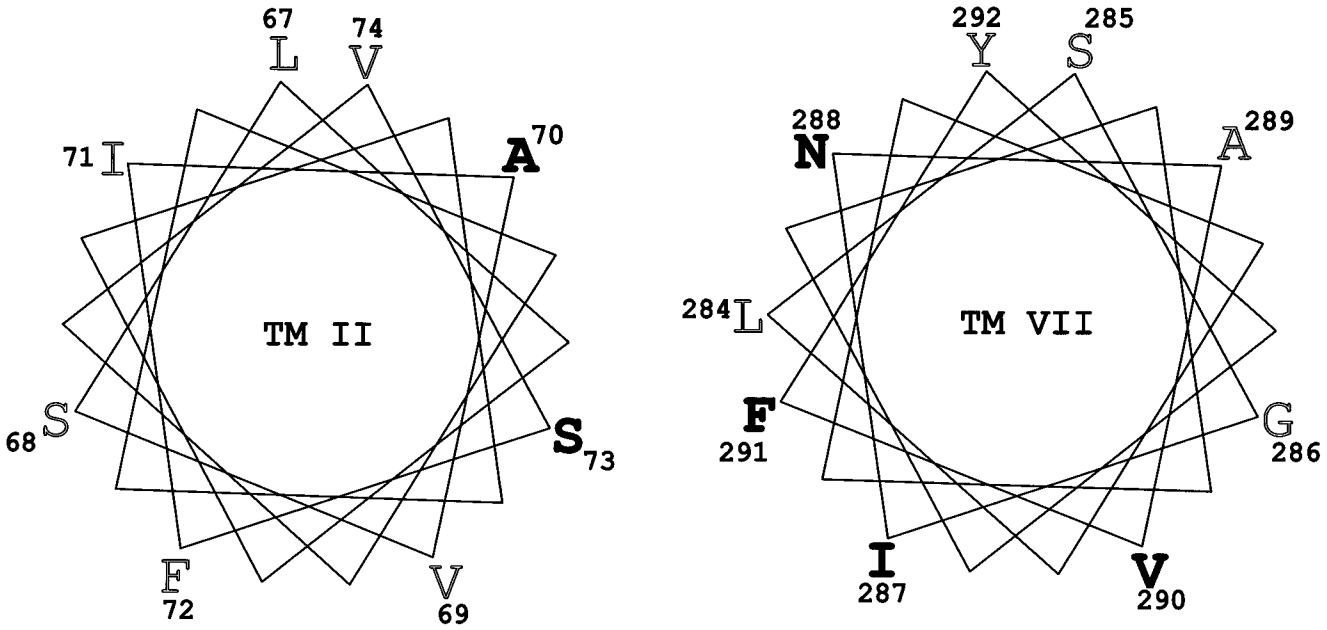

FIGURE 3: Helical wheel plot of residues in the second or seventh transmembrane segment. Residues of TM II or residues of TM VII changed by cysteine-scanning mutagenesis were plotted on a helix wheel and are indicated by the single-letter code. Positions of residues sensitive to pCMBS treatment are shown as bold letters.

the first cytoplasmic loop, whereas the α/β structure model assumes these residues are within the membrane environment. The observation that S73C is an extremely pCMBS-sensitive mutant particularly contributes to the following discussion about how the different models are consistent with the experimental data.

The observation that pCMBS can interact with particular intramembranous cysteine residues, whereas other SH groups (presumably because of the hydrophobic environment) are excluded from accessibility, led to the question of how a highly permeable thiol reagent like NEM would influence transport activity, especially of those mutants that were resitant to pCMBS. To investigate the role of individual SH groups in transport inhibition by NEM, 3-*O*-methyl-D-glucose instead of 2-deoxy-D-glucose was used as it is known that NEM in cells inhibits the hexokinase reaction (*23*). Regarding the first EL, the data in Table 2 indicate that NEM inhibited transport in the Cys-replacement mutants from 0 to about 90% (N- to C-terminal direction). These data confirmed our previous observation that the inhibitory effect caused by modification of SH groups decreased with increasing distance from the flanking transmembrane segment. It is noteworthy that L67C and S68C belong to those transmembrane mutants whose transport was only slightly inhibited by NEM (86 and 87% retained activity, respectively). On the other hand, cysteine at position 69, which is located at a pCMBS-restricted site of the helix, was extremely sensitive to the membrane-permeant transport inhibitor (2% retained activity). Residues at position 70 and 73 were located in parts of the α-helix that were accessible to both the permeable and the membrane-impermeant sulfhydryl-reactive agents.

Cysteine-Scanning Mutagenesis of the Seventh TM−Fourth EL Region. Figure 2 indicates that replacement of Tyr-293 (at the N-terminal end of the fourth EL) or Tyr-292 (at the C-terminal end of the seventh TM) with cysteine residues decreased 2-deoxy-D-glucose uptake rates each by 76%. In addition, substitution of cysteine for Gly-286 and Asn-288 in the seventh TM almost eliminated transport activity entirely. Transport activities of the G286C and N288C mutants were only 8 and 13%, respectively, compared with the nonmutated Cys-less GLUT1 if 2-deoxy-D-glucose uptake rates were normalized to the relative amount of transporter protein in total membrane fractions (for details, see Materials and Methods). All other residues could be replaced by cysteine-scanning mutagenesis with respect to transport activity. Regarding the membrane-adjacent region of the fourth EL, data from Table 1 indicate that pCMBS most effectively impaired 2-deoxy-D-glucose uptake if cysteine residues were localized close to the loop−membrane boundary; Y293C, however, appeared to be less sensitive than S294C (42 vs 7% retained activity, respectively). Consistent with the observation from the first EL, the thiol group farthest from the transmembrane segment (Cys-297) led to a tremendous increase in 2-deoxy-D-glucose uptake (323%) after pCMBS treatment that could be reversed by cytochalasin B (data not shown).

Regarding transmembrane residues at the C-terminal end of the seventh TM, nine residues in a row were individually changed by cysteine-scanning mutagenesis (see Figure 1). The data in Table 1 indicate that at least four cysteine residues of this membrane domain were accessible to pCMBS since transport activities of cysteine-substitution mutants I287C, N288C, V290C, and F291C were markedly inhibited (i.e., 7, 14, 44, and 9% retained activities, respectively). In contrast, pCMBS increased the extremely low transport activity of the G286C mutant by 3-fold; the stimulation could be prevented by cytochalasin B (data not shown). Drawn on a helix wheel, pCMBS-sensitive amino acid residues within this portion of the seventh TM lie on the same facial half of the helix (see Figure 3).

NEM treatment of mutants whose thiol groups were inserted into the fourth EL confirmed the observation made after pCMBS application that transport inhibition decreased when the distance between the SH groups and the membrane boundary increased (shown in Table 2). Consistent with data

Table 2: Effect of NEM on Cys-Replacement Mutants[a]

region	Cys-replacement mutants	% activity ± SD	no. of oocytes
first EL	T62C	81 ± 24	88
	T63C	105 ± 20	55
	L64C	77 ± 21	59
	W65C	78 ± 24	59
	S66C	8 ± 7	78
second TM	L67C	86 ± 13	60
	S68C	87 ± 16	88
	V69C	2 ± 5	79
	A70C	20 ± 10	44
	I71C	78 ± 36	58
	F72C	nd	30
	S73C	15 ± 9	88
	V74C	78 ± 43	86
seventh TM	L284C	76 ± 21	89
	S285C	90 ± 35	88
	G286C	210 ± 425	73
	I287C	15 ± 39	60
	N288C	28 ± 37	57
	A289C	81 ± 23	61
	V290C	47 ± 20	63
	F291C	2 ± 4	43
	Y292C	49 ± 25	89
fourth EL	Y293C	37 ± 31	60
	S294C	6 ± 13	59
	T295C	61 ± 31	90
	S296C	92 ± 28	72
	I297C	204 ± 61	59

[a] Water-injected *Xenopus* oocytes and oocytes expressing single-cysteine mutants were incubated with 10 mM NEM at room temperature for 60 min. Thereafter, uptake of tritium-labeled 3-*O*-methyl-D-glucose was assessed as described in Materials and Methods. For each single-cysteine-replacement mutant, the retained transport activity after NEM treatment was expressed as a percentage of the 3-*O*-methyl-D-glucose transport rate in the absence of NEM. Uptake rates obtained from water-injected *Xenopus* oocytes were subtracted. For single-Cys-replacement mutants, values are the mean percentage ± standard deviation of retained uptake rates and the total number of single *Xenopus* oocytes from two or three independent experiments. nd means not detected.

from pCMBS-sensitivity scanning, covalent modification by NEM of the cysteine residue at position 297 resulted in stimulation of transport by a factor 2. With respect to identification of the seventh TM−fourth EL boundary, NEM caused an almost equal inhibition of transport activities of the Y293C (fourth EL) and Y292C (seventh TM) mutants, whereas pCMBS failed to inhibit transport induced by Y292C. For the majority of membrane-harbored residues in TM VII, however, the ability of NEM to inhibit glucose transport was similar to that observed after pCMBS treatment. This statement is also valid for the stimulatory effect by NEM on the G286C mutant-induced uptake rates (210% increase).

DISCUSSION

Site-Directed and Cysteine-Scanning Mutagenesis. To investigate the local secondary structure within defined portions of GLUT1 and, in particular, to identify those residues that form the end points of external loops and putative transmembrane segments, we used a GLUT1 mutant that was devoid of cysteine residues. The cysteine-less version of GLUT1 (Cys-less GLUT1) fortunately functioned as an active transport protein (*13*−*15*). Thus, the reactivity of single thiol groups was introduced into protein domains of the Cys-less GLUT1 that include the flanking regions of the external loop and transmembrane segment. Modification of single inserted cysteine residues by extracellular pCMBS, whose distribution is restricted to the aqueous phase, was the basis for probing the exact limits of external loops and transmembrane segments. In addition, the highly permeable SH reagent NEM was used to address the role of individual residues in transport inhibition independent of their accessibility to the aqueous phase.

Following cysteine substitution of single loop serine residues adjacent to the flanking transmembrane segment, pCMBS treatment-induced transport inhibition of >90% exclusively occurred in mutants whose thiol groups were present in EL I and IV, respectively. By coincidence, glycosylation-scanning mutagenesis experiments suggested that the second and third ELs of GLUT1 are not necessarily involved in the transport process (*10*). Thus, cysteine-scanning mutagenesis was carried out at the flanking regions of the first EL−second TM and seventh TM−fourth EL boundaries. The majority of amino acids could be replaced with respect to transport. Considering previously published site-directed mutagenesis results at this domain, Trp-65 could be replaced by either glycine or leucine (*21*), supporting the notion that tryptophan at this position can be changed to a number of other amino acids without a change in the transport activity. The change of phenylalanine at position 72 reduced transport activity to almost zero. Normalized to the relative amount of F72C mutant protein in total membrane fraction, the mean uptake rate was only 8% compared with that of the nonmutated Cys-less GLUT1. Further experiments are needed to determine whether the loss of phenylalanine per se or the particular change to cysteine residues accounts for transport inactivation. Elucidating the particular role of aromatic amino acids in the transport activity of this helix is an attractive goal of future investigations because, in addition to Phe-72, TM II contains two more phenyalanine residues at positions 81 and 86.

In the fourth EL−seventh TM region, including residues Leu-284−Iso-297, four cysteine-replacement mutants displayed 2-deoxy-D-glucose uptake rates that were less than 50% of that of the nonmutated Cys-less GLUT1. The literature suggests that the tyrosine residues at positions 292 and 293 play an active role in transport since replacement with phenylalanine reduced their relative intrinsic activities to 50 and 80% of that of wild-type GLUT1, respectively (*24*). If isoleucine was introduced in place of Tyr-293, V_{max} for 2-deoxy-D-glucose was markedly reduced, and in addition, a dramatic (300-fold) reduction in affinity for the endofacial transport inhibitor cytochalasin B was observed (*25*). In the Cys-less GLUT1, individual substitution of cysteine for tyrosine at each position led to reduction of transport activity by 76%. Site-directed replacement of these tyrosine residues with a different aromatic amino acid seems not to be sufficient to maintain full transport activity; impairment of transport, however, was moderate compared with the decrease in uptake rates due to a single change of a tyrosine to a cysteine. The importance of this loop for glucose transport was supported by recent data showing that substitution of alanine for Ser-310 and Thr-311 in GLUT4, corresponding to positions 294 and 295 in GLUT1, respectively, suppressed transport activity (*26*). Binding and photolabeling experiments suggest that substitution of each

of these residues locks the transporter in an outward-facing conformation. In the Cys-less GLUT1, Ser-294 and Thr-295 could be replaced however with respect to transport since substitution by cysteine residues did not reduce (Thr-295) or only marginally (Ser-294) reduced transport activity. In the putative transmembrane segment, the transport activities of two other single cysteine mutants, i.e., G286C and N288C, were also markedly reduced, indicating that glycine and asparagine are irreplaceable residues.

pCMBS-Sensitivity Scanning. Regarding the flanking segments at the first EL−second TM boundary, pCMBS exerted dramatic transport inhibition if the SH group was present at the putative C-terminal limit of the loop (position 66). It is important to note that the respective counterpart on the membrane side (position 67) did not respond to pCMBS application. Prediction of the exact limits however was hindered by the fact that NEM treatment led to results comparable to those for the pCMBS effect, suggesting that leucine 67 does not play a major role in the transport process. When the other loop cysteine residues were tested, pCMBS sensitivities decreased with increasing distance from the membrane boundary, and the N-terminal end point thiol group even led to transport stimulation of the mutant transporter. It is tempting to speculate that loop residues proximal to the membrane segments play a more critical role in the transport process than those that are farther from the membrane helix. This may be due to their preferred role in the restraint of flexibility of helix arrangement necessary for conformational changes. The reason the most distal cysteine residue led to transport stimulation after pCMBS treatment remains an open question.

Since the GLUT1 protein is largely accessible to water, as concluded from deuterium exchange experiments (*27*, *28*), scanning of pCMBS sensitivity provided useful information with respect to the secondary structure of transmembrane segments. Helical turns presumably place Val-69 into a position that is partly restricted from reaction with pCMBS but fully accessible to NEM. Thiol groups at positions 70 and 73 were accessible without restriction to both pCMBS and NEM. Consistent with the view that the residues at positions 67−74 are part of a helical structure, pCMBS-sensitive residues, when drawn on a helix wheel, are positioned on the same face of the helix. With respect to the exact limits of the membrane helix or flanking external loop, predictions deduced from hydropathy plots are consistent with the experimental data because distinct pCMBS sensitivities were observed for L67C and S66C with the stipulation that the thiol group of the transmembrane segment could be accessible to pCMBS without leading to transport inhibition. Even if pCMBS is capable of reaching residues in transmembrane segments, as also was anticipated for the alternative topology models, data obtained from pCMBS-sensitivity scanning of the putative first external loop are not characteristic of a membrane α-helix or a β-strand structure.

Regarding the flanking regions at the fourth EL−seventh TM boundary, remarkable inhibitory effects caused by pCMBS and NEM were observed for those cysteines that are located in the N-terminal limit of the loop. Also like the results from the first EL, but even more pronounced, was the stimulation of transport induced by thiol groups located a few positions from the transmembrane segment. With respect to these loop positions, one can speculate that pCMBS is able to induce structural changes that are advantageous to conformational changes. Addressing the boundaries of loop and transmembrane segments in this region, we faced the difficulty that transport activities after individual replacement of the tyrosine residues at positions 292 and 293 were remarkably low, displaying only 24% of that of the nonmutated Cys-less GLUT1. Despite this caveat, the pCMBS sensitivity was demonstrated for the end point residue of the loop but was almost absent for the counterpart in the putative transmembrane segment. Conversely, the difference in NEM sensitivities of both residues was only marginal (37% retained transport activity for Y293C vs 49% retained transport activity for Y292C). This inhibition pattern suggests that the transition between the membrane-spanning segment and the external loop is between Tyr-292 and Tyr-293, as predicted from the hydropathy plot. In the postulated transmembrane portion of the mutated amino acid stretch, the inhibitory effects exerted by pCMBS or NEM were surprisingly similar. Helical wheel drawing demonstrated that the pCMBS-sensitive residues lie on the same facial half of the helix. Transport stimulation of G286C induced by pCMBS or NEM has to be interpreted with caution since the transport activity of the untreated mutant was less than 10% of that of the nonmutated Cys-less GLUT1. Cytochlasin B-mediated inhibition however indicated that the stimulation of 2-deoxy-D-glucose uptake was due to an increase in transport activity of the mutant transporter. One might speculate that pCMBS would compensate for changes due to the loss of the nonpolar hydrophobic glycine by interaction with the cysteine residue.

Compatibility of Alternative Membrane Topology Models with Experimental Data. Results from pCMBS-sensitivity scanning have been mainly considered in light of the 12-helix membrane topology. Since there are good arguments in favor of two alternative secondary structure models (*2*, *3*), i.e., the 16-β-strand (16-TM) or the α/β structure model with 14 transmembrane segments (14-TM), determining how these proposed structures are consistent with our experimental data was of particular interest.

(a) In both alternative topology models, the first EL−second TM region containing residues 62−74 (see Figure 1) is predicted to be partially (16-TM) or entirely (14-TM) part of the second TM. The residues at positions 65 and 66, which in the 12-helix model are located at the C-terminal end of the first loop, are both inhibited by pCMBS. In a β-barrel structure, it is less likely that two adjacent residues are affected by a membrane-impermeant inhibitor like pCMBS. Furthermore, the transport activity of the mutant that carries the cysteine residue at position 73 was dramatically inhibited by pCMBS treatment (3% remaining activity). The 16-TM model, however, predicts that this residue is part of the first cytoplasmic loop. We know from single-cysteine mutants of wild-type GLUT1 that the external application of pCMBS failed to affect glucose transport if the exofacially exposed Cys-429 was removed, although all other cysteines, including one cytoplasmic loop residue, were still present (*8*).

(b) The pCMBS-induced transport inhibition by modification of thiol groups at positions 62−66, representing external loop residues in the 12-helix model, was characteristic in that the increase in pCMBS sensitivity correlates with the

closer location of thiol groups to the transmembrane segment limit. Regarding the alternative topology models, accessibility of inserted thiol groups to pCMBS would steadily increase from the membrane periphery toward the middle of the second transmembrane segment.

(c) Both alternative topology models assume that the entire amino acid stretch containing the seventh TM−fourth EL region (residues 284−297) is part of an external loop. This prediction must explain the characteristic pattern of pCMBS-sensitivity scanning exhibiting alternation of sensitive and insensitive thiol groups at positions 284−292 (transmembrane segment in the 12-helix topology) and, in addition, the continuous decline in inhibition by pCMBS for positions 293−297 (loop segment in the 12-helix model). Moreover, positions 292 and 293 were affected differently by pCMBS which is consistent with the respective end points of loop and transmembrane segment.

We are aware of the fact that the transmembrane helices may extend beyond the membrane and form part of the loop structure. Thus, the partition of the entire amino acid stretch into two sections, one containing the alternating pCMBS sensitivities assigned to the membrane helix and the other displaying decreasing pCMBS sensitivities assigned to the external loop structure, may be an oversimplification. Taken together, the pCMBS-sensitivity scanning data at two different locations of GLUT1, however, are more consistent with the 12-helix membrane topology than with the two alternative secondary structure models.

REFERENCES

1. Mueckler, M., Caruso, C., Baldwin, S. A., Panico, M., Blench, I., Morris, H. R., Allard, W. J., Lienhard, G. L., and Lodish, H. F. (1985) *Science 229*, 941−945.
2. Fischbarg, J., Cheung, M., Czegledy, F., Li, J., Iserovich, P., Kuang, K., Hubbard, J., Garner, M., Rosen, O. M., Golde, D. W., and Vera, J. C. (1993) *Proc. Natl. Acad. Sci. U.S.A. 90*, 11658−11662.
3. Ducarme, P., Rahman, M., Lins, L., and Brasseur, R. (1996) *J. Mol. Model. [Electronic Publication] 2*, 27−45.
4. Cairns, M. T., Alvarez, J., Panico, M., Gibbs, A. F., Morris, H. R., Chapman, D., and Baldwin, S. A. (1987) *Biochim. Biophys. Acta 905*, 295−310.
5. Davies, A., Meeran, K., Cairns, M. T., and Baldwin, S. A. (1987) *J. Biol. Chem. 262*, 9347−9352.
6. Baldwin, S. A. (1992) *Biochem. Soc. Trans. 20*, 533−537.
7. May, J. M., Buchs, A., and Carter-Su, C. (1990) *Biochemistry 29*, 10393−10398.
8. Wellner, M., Monden, I., and Keller, K. (1992) *FEBS Lett. 309*, 293−296.
9. Kasahara, T., and Kasahara, M. (1997) *Biochim. Biophys. Acta 1324*, 111−119.
10. Hresko, R. C., Kruse, M., Strube, M., and Mueckler, M. (1994) *J. Biol. Chem. 269*, 20482−20488.
11. Frillingos, S., Sahin-Toth, M., Persson, B., and Kaback, H. R. (1994) *Biochemistry 33*, 8074−8081.
12. Frillingos, S., Sun, J., Gonzales, A., and Kaback, H. R. (1997) *Biochemistry 36*, 269−273.
13. Due, A. D., Cook, J. A., Fletcher, S. J., Zhi-Chao, Q., Powers, A. C., and May, J. M. (1995) *Biochem. Biophys. Res. Commun. 208*, 590−596.
14. Wellner, M., Monden, I., and Keller, K. (1995) *FEBS Lett. 370*, 19−22.
15. Mueckler, M., and Makepeace, C. (1997) *J. Biol. Chem. 272*, 30141−30146.
16. Bowie, J. U. (1997) *J. Mol. Biol. 272*, 780−789.
17. Mueckler, M., and Lodish, H. F. (1986) *Cell 44*, 629−637.
18. Krieg, P. A., and Melton, D. A. (1984) *Nucleic Acids Res. 14*, 7057−7070.
19. Deng, W. P., and Nickoloff, J. A. (1992) *Anal. Biochem. 200*, 81−88.
20. Keller, K., Strube, M., and Mueckler, M. (1989) *J. Biol. Chem. 264*, 18884−18889.
21. Garcia, J. C., Strube, M., Leingang, K., Keller, K., and Mueckler, M. (1992) *J. Biol. Chem. 267*, 7770−7776.
22. Wellner, M., Monden, I., Mueckler, M., and Keller, K. (1995) *Eur. J. Biochem. 227*, 454−458.
23. D'Amore, T., and Lo, T. C. Y. (1986) *J. Cell. Physiol. 127*, 106−113.
24. Mueckler, M., Weng, W., and Kruse, M. (1994) *J. Biol. Chem. 269*, 20533−20538.
25. Mori, H., Hashiramoto, M., Clark, A. E., Yang, J., Muraoka, A., Tamori, Y., Kasuga, M., and Holman, G. D. (1994) *J. Biol. Chem. 269*, 11578−11583.
26. Doege, H., Schürmann, A., Ohnimus, H., Monser, V., Holman, G. D., and Joost, H. G. (1998) *Biochem. J. 329*, 289−293.
27. Jung, E. K. Y., Chin, J. J., and Jung, C. Y. (1986) *J. Biol. Chem. 261*, 9155−9160.
28. Alvarez, J., Lee, D. C., Baldwin, S. A., and Chapman, D. (1987) *J. Biol. Chem. 262*, 3502−3509.

BI980440R